Shape and energetics of DNA plectonemes

Prashant K. Purohit

Abstract The mechanics of DNA at length scales of few hundred nanometers is described by a fluctuating elastic rod model. In this paper we couple the fluctuating rod model with a variational method for describing plectonemes to unravel the mechanics of some recent single molecule experiments. We are able to reproduce some features seen in these experiments which analyze plectoneme formation in DNA under tension by continuously twisting it and tracking its end-to-end distance, torque, etc., as a function of the added link. Our model accounts for configurational entropy and electrostatics in the plectoneme. We find that configurational entropy makes a significant contribution to the mechanics of the plectoneme while electrostatics (in the presence of monovalent counterions) plays a relatively minor role.

1 Introduction

It is now well established that double-stranded DNA behaves as a thermally fluctuating elastic rod at length-scales of a few hundred nanometers [9, 12]. The mechanical properties of DNA at these length scales have been measured by various techniques, including single molecule experiments, and it is known that the average bending modulus of a random sequence of DNA bases is about $K_b = 205\text{pNnm}^2$ [9]. Single moleucle techniques have also established that the twisting modulus of DNA is around $K_t = 431\text{pNnm}^2$ [12]. The fact that DNA is a twist storing polymer allows it to form plectonemes when its linking number Lk is large. In fact, bacterial cells store DNA in the form of plectonemes in order to pack the their long genome into the small volume within their cell walls. As a result retrieval of genetic information from the DNA requires molecular machines to manipulate the plectonemes by exerting forces and torques on them [14]. The plectonemes themselves have small radii so that DNA electrostatics can also have an important role in the mechanics.

Prashant K. Purohit
University of Pennsylvania, Philadelphia. PA 19014, USA. e-mail: purohit@seas.upenn.edu

This motivates our study of the mechanics of DNA plectonemes with the effects of configurational entropy and electrostatics.

Plectonemes in elastic rods have been studied by many authors [3, 5, 8, 15, 18]. A brief review of the research in this subject can be found in Purohit (2008) [15] who show that many of the features seen in recent single molecule experiments of Forth *et al.* (2008) [6] on DNA plectonemes can be qualitatively reproduced using an elastic rod model. In Purohit (2008) [15] plectonemic shapes are obtained by combining helical and localizing solutions of the equations of the balance of forces and moments for an elastic rod. This approach was first used by Stump *et al.* (1998) [16] to describe 'balanced ply' structures in rods and extended by various authors to describe 'variable plys' [5], 'generalized plys' [18] as well as plectonemes and DNA plasmids. The approach of Purohit (2008) [15] based on balance of forces and moments is kinematically constrained since helices of constant radius and pitch are inserted into non-planar localizing solutions of rods to obtain plectonemic solutions. On the other hand, Clauvelin *et al.* (2008) [3] and van der Heijden *et al.* (2003) [18] use a variational formulation to solve for the geometry of the plectoneme, and Clauvelin *et al.* (2008) apply their methods to interpret magnetic tweezer experiments on DNA plectonemes. One of our goals in this paper is to show that both these methods lead to exactly the same results for the parameters of the plectoneme if the energy of the helices in the variational formulation is constrained to constant helical radius and pitch. The variational method is, of course, more general than the method of Purohit (2008) [15] since it can be applied to plectonemes with a varying helical pitch, and can also be easily extended to account for entropy and electrostatics. In fact, we use the variational method to determine the entropic and electrostatic corrections to geometrical parameters of the plectonemes. We show that configurational entropy has a larger effect on the plectoneme geometry than electrostatics, but both represent only small deviations from the elastic rod solution.

2 Review of Kirchhoff's theory of rods

In Kirchhoff's theory the coordinates of the center-line of a rod are given by a position vector $\mathbf{P}(s)$ where s is the arc-length along the rod. At each point s of the rod we attach a coordinate frame called the material frame. The unit vectors of the material frame are denoted by $\mathbf{d}_1(s)$, $\mathbf{d}_2(s)$, $\mathbf{d}_3(s)$ with $\mathbf{d}_3(s)$ chosen to be along the tangent to the rod at every point so that $\mathbf{d}_3(s) = \mathbf{P}'(s) = \frac{d\mathbf{P}(s)}{ds}$. Note that the tangent $\mathbf{P}'(s)$ is a unit vector since the rod is assumed to be inextensible. The derivatives of these vectors along the arc-length s contain information about the local curvature of the rod. In particular,

$$\frac{d\mathbf{d}_i}{ds} = \boldsymbol{\kappa} \times \mathbf{d}_i, \qquad \text{for} \quad i = 1,2,3, \tag{1}$$

where $\boldsymbol{\kappa}(s) = [\kappa_1(s) \quad \kappa_2(s) \quad \kappa_3(s)]$ is the curvature vector. The internal moment $\mathbf{M}(s)$ at any point on the rod is given by

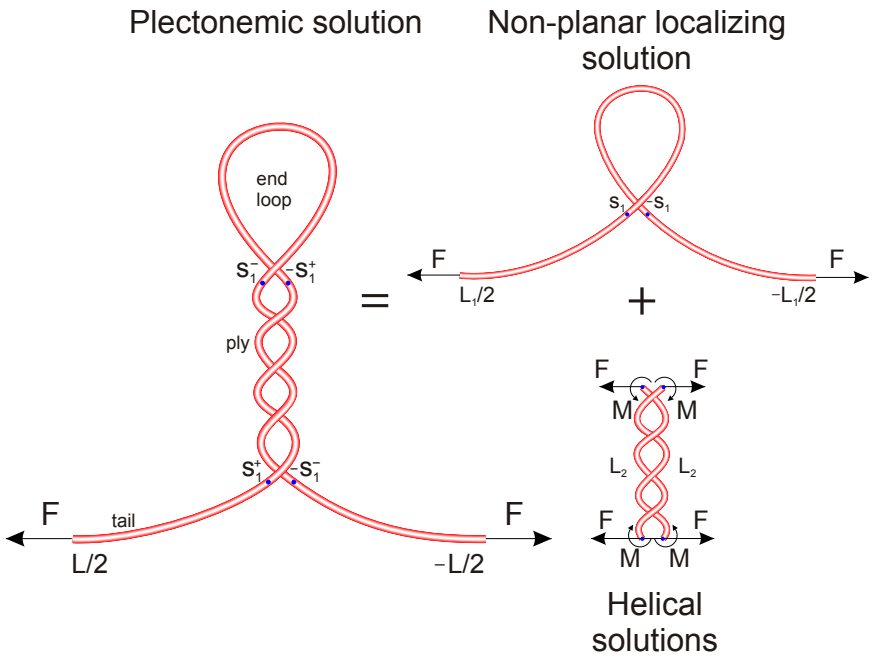

Fig. 1 Constructing a plectoneme. First, the localizing solution is cut at $\pm s_1$. Then, the end loop and the two tails are separated vertically. And finally, two helices with integer number of turns are inserted in between, so as to ensure continuity of the displacement, tangent and curvature at $\pm s_1$. The torsion of the centerline of the rods is not required to be continuous at $\pm s_1$. This figure is reproduced from Purohit (2008) [15].

$$\mathbf{M} = K_b \kappa_1 \mathbf{d}_1 + K_b \kappa_2 \mathbf{d}_2 + K_t \kappa_3 \mathbf{d}_3, \tag{2}$$

where K_b and K_t are the bending and twisting moduli of the DNA. The equations for the balance of forces and moments in the rod are then simply,

$$\frac{d\mathbf{F}}{ds} = \mathbf{0}, \qquad \frac{d\mathbf{M}}{ds} + \mathbf{d}_3 \times \mathbf{F} = \mathbf{0}, \tag{3}$$

where $\mathbf{F}(s)$ is the internal force in the rod. A special class of solutions to the balance equations are helices which have curvature $\kappa = [\kappa_1 \quad \kappa_2 \quad \kappa_3]$ and Frenet torsion τ that satisfy a simple vector equation

$$\mathbf{F} = (K_t \kappa_3 - K_b \tau)[\kappa_1 \mathbf{d}_1 + \kappa_2 \mathbf{d}_2 + \tau \mathbf{d}_3], \tag{4}$$

where $\mathbf{d}_3(s) = \mathbf{P}'(s)$ is the tangent vector and $\mathbf{F}$ is a constant force [13]. Note that the balance equations imply that $\mathbf{F}(s)$ is constant along the rod and its value is determined by the external force applied on the DNA, which in the experiments considered in this paper, are applied using an optical tweezer setup [6]. Following Nizette and Goriely (1999) [13] we will assume that the laboratory coordinate frame

is chosen in such a way as the applied force $\mathbf{F}$ is aligned with the z-axis so that $\mathbf{F}(s) = F\mathbf{e}_z$. The position vector $\mathbf{P}(s)$ is then explicitly written as

$$\mathbf{P}(s) = R(s)\cos\Phi(s)\hat{\mathbf{e}}_x + R(s)\sin\Phi(s)\hat{\mathbf{e}}_y + Z(s)\hat{\mathbf{e}}_z, \tag{5}$$

where we have used a cylindrical coordinate system. Analytical solutions for $R(s)$, $\Phi(s)$ and $Z(s)$ (which are more general than helices) are known in terms of elliptic functions and elliptic integrals and can be found in Nizette and Goriely (1999) [13].

3 Localizing solutions

A special case of the general solution, the non-planar localizing solution, is appropriate for describing some of the equilibria in single-molecule experiments and is given by

$$Z(s) = z_3 s - \lambda(z_3 - z_1)E(\frac{s}{\lambda}|k), \tag{6}$$

$$Z'(s) = z_1 + (1 - z_1)\mathrm{sn}^2(\frac{s}{\lambda}|k), \tag{7}$$

$$\frac{M_3\lambda}{K_b} = \frac{M_z\lambda}{K_b} = \sqrt{(1+z_1)(1+z_3)}, \tag{8}$$

where $k^2 = \frac{1-z_1}{z_3-z_1}$, $\mathrm{sn}(u|k)$ is an elliptic function (see below) and $E(u|k)$ is the incomplete elliptic integral of the second kind defined as follows (for details, see Abramowitz and Stegun (1964) [1]):

$$E(u|k) = \int_0^u (1 - k^2\mathrm{sn}^2(x|k))\,dx, \qquad \text{where} \quad \mathrm{sn}(x|k) = \sin\varphi,$$
$$\text{and} \quad x = \int_0^\varphi \frac{d\theta}{\sqrt{1 - k^2\sin^2\theta}}. \tag{9}$$

In the solution given above $\lambda = \sqrt{\frac{K_b}{F}}$ is determined immediately since the force F is prescribed. The remaining constants z_1 and z_3 are determined from the known value of the applied torque M_3 (or the linking number ΔLk) and the condition that $Z'(\pm\frac{L}{2}) = 1$ which says that the tangents at the two ends of the rod are aligned with the z-axis in the laboratory frame. The resulting boundary condition is

$$1 = z_1 + (1 - z_1)\mathrm{sn}^2(\frac{L}{2\lambda}|k). \tag{10}$$

The solution obtained from these equations gives us the bent and twisted shape of the rod for $\frac{2L\sqrt{K_bF}}{K_t} < 2\pi$. Plectoneme formation occurs when $\frac{2L\sqrt{K_bF}}{K_t} > 2\pi$ and Purohit (2008) [15] show how to construct these solutions by combining helical solutions of the rod with the non-planar localizing solutions in such a way that the balance of

forces and moments is satisfied at each point along the rod. A brief summary of the procedure is given below since the notation from this section will also be used to describe the variational formulation.

4 Constructing the plectonemic solution

We assume that the total length of the rod is L and the length eaten up by the helical region is $2L_2$ so that $L_1 = L - 2L_2$ is the leftover length that (without the helices) corresponds to a shape described by the non-planar localizing solution (see figure 1). At present L_1 is an unknown and so are $\pm s_1$ (with $-\frac{L_1}{2} < -s_1 < 0 < s_1 < \frac{L_1}{2}$) which are the arclengths at which we cut the rod to insert the plectonemic helices. The arclength interval $[-s_1, s_1]$ corresponds to the end loop while the intervals $[-\frac{L_1}{2}, -s_1]$ and $[s_1, \frac{L_1}{2}]$ correspond to the tails with the ends $s = \pm\frac{L_1}{2}$ where the tension F is applied. The center-line of the helix is given by $\mathbf{P}(s) = [r\cos(As+B) \quad Qs+D \quad r\sin(As+B)]$ where A, B, Q, D and r are all constants and we require $A^2r^2 + Q^2 = 1$ to enforce inextensibility. The length of each of the helices is $L_2 = 2\pi mr\sec\alpha$ where α is the pitch angle ($\tan\alpha = \frac{Q}{Ar}$) and m is the number of turns in each helix. Fuller (1971) [7] showed that the writhing number for this plectonemic solution (completed to a closed curve) is $2m\sin\alpha$. Assuming that $\kappa_3 = \frac{M_3}{K_t}$ is the constant twist rate in the rod in the post-buckled shape, the total link stored in the rod can be obtained from the Fuller-White-Calugrenau relation which is equated to the prescribed change in link, ΔLk, leading to:

$$\Delta Lk = \frac{M_3 L}{2\pi K_t} + 2m\sin\alpha, \tag{11}$$

$$L = L_1 + 4\pi mr\sec\alpha, \tag{12}$$

where the second equation merely says that the length in the helices and the localizing solution should add up to the total length L.

The Frenet curvature and torsion [13] of the helix are respectively $\kappa = A^2 r$ and $\tau = AQ = A\sqrt{1-A^2r^2}$. s_1 is the arclength at which the rod solution intersects the helix. We require continuity of the tangent at this point. This can be enforced if we find a point s_1 in the rod solution with $0 < s_1 < L_1$, such that

$$X(s_1)X'(s_1) + Z(s_1)Z'(s_1) = \frac{d}{ds}(X^2(s) + Z^2(s))|_{s_1} = 0. \tag{13}$$

If there exists such a point s_1 in the localizing solution then the parameters A, B, D, Q and r for the helix can be uniquely determined using

$$r^2 = X^2(s_1) + Z^2(s_1), \qquad Q = Y'(s_1), \qquad A^2 = \frac{1 - Y'^2(s_1)}{X^2(s_1) + Z^2(s_1)}. \tag{14}$$

We also need to satisfy continuity of forces and moments at s_1. For a helix the balance of forces and moments can be summarized by the single vector equation (4) in the material frame [13]. In writing this equation we assume that there are no contact or interaction forces (for instance, electrostatic) between the helices in the DNA plectoneme. This seems like a good assumption if the radius and pitch of the helices is much larger than the diameter of DNA (about 2nm) and there is no self intersection. It is difficult to verify these criteria in an experiment. However, we show in what follows that the calculated helix radii and pitch under the assumption of no self-contact and no interaction are indeed larger than 4nm for the range of forces considered in this paper. In other words, the solutions are consistent with the assumption. For a discussion of the balance equations of rods with self-contact we refer the reader to an article by van der Heijden *et al.* [19]. Quantitative treatment of the contact force in DNA plectonemes has also been peformed by Clauvelin *et al.* [3]. Later in this paper we relax the assumption of no interaction between the helices and consider the electrostatic interaction energy and the entropic cost of constrained fluctuations due to the helical geometry. Going back to (4) and taking magnitudes on both sides we get

$$F = (K_t\kappa_3 - K_b\tau)\sqrt{\kappa_1^2+\kappa_2^2+\tau^2}. \tag{15}$$

Now, for any equilibrium solution of a Kirchhoff rod we know that M_3 and M_z are constants independent of s. We exploit this fact in the helical solution and note that

$$|K_b\kappa_1\mathbf{d}_1 + K_b\kappa_2\mathbf{d}_2|^2 = |\mathbf{M} - M_3\mathbf{d}_3(s_1)|^2 = M_3^2|\mathbf{e}_z - \mathbf{d}_3(s_1)|^2 = 2M_3^2(1-Z'(s_1)). \tag{16}$$

Substituting this result back into (15) and remembering that the force and moment have to be continuous at s_1 we obtain

$$1 = (\frac{M_3\lambda}{K_b} - \tau\lambda)\sqrt{\frac{2M_3^2\lambda^2}{K_b^2}(1-Z'(s_1)) + \tau^2\lambda^2}. \tag{17}$$

Equations (11), (12), (13) and (17) together with the following are six equations for the six unknowns – L_1, s_1, m, z_1, z_3 and M_3 – in the plectonemic solution.

$$\frac{M_3\lambda}{K_b} = \sqrt{(1+z_1)(1+z_3)}, \qquad \frac{L_1}{2\lambda} = K(\frac{1-z_1}{z_3-z_1}). \tag{18}$$

These six equations are solved using Newton's method. For a given value of F and material properties K_b and K_t, the helix parameters A, Q, r etc., can then be obtained from (14) and L_1 and m can be determined using (11) and (12). This completely determines a plectonemic shape.

5 Variational method

The shape of the plectoneme in the above method is obtained by solving (4) which represents the balance of forces and moments in the helix. The helix parameters can also be obtained by a variational method which is general enough to account for electrostatic and entropic interactions [10] as well as varying pitch angle $\alpha(s)$ of the helix [18]. In brief, the electrostatic interaction given by Marko and Siggia (1995) [10] is obtained by solving the Poisson-Boltzmann (or Debye-Huckel) equation for two parallel negatively charged cylindrical DNA molecules placed a certain distance apart in a solution containing monovalent counterions. According to Marko and Siggia (1995) [10] the electrostatic interaction energy is significant if the distance between the DNA molecules is in the range of 1-3nm. The entropic cost of confining the DNA to a helix is obtained by putting a limit on the amplitude of thermal fluctuations so that self-intersection of the helices is not allowed [10]. To see how to write down the energy in our problem after taking electrostatics and entropy into account we observe that

$$\kappa_1^2+\kappa_2^2=\alpha'^2+\frac{1}{r^2}\cos^4\alpha, \qquad \kappa_3=\phi'+\frac{1}{r}\cos\alpha\sin\alpha, \tag{19}$$

where ϕ is internal twist angle of $\mathbf{d}_2$ (or $\mathbf{d}_1$) about the tangent $\mathbf{d}_3$ [18]. We express the energy stored in the plectonemic helices as

$$V=\int_0^{L_2}\mathscr{L}(\alpha,\alpha',\phi,\phi')\,ds, \tag{20}$$

where L_2 is the length of each helix in the plectoneme and $\mathscr{L}$ is the energy per unit length of each helix which is given by

$$\begin{aligned}\mathscr{L}=&\frac{K_b}{2}\left(\alpha'^2+\frac{1}{r^2}\cos^4\alpha\right)+\frac{K_t}{2}\left(\phi'+\frac{\sin 2\alpha}{2r}\right)^2+\frac{k_BT}{A^{1/3}(\pi r\tan\alpha)^{2/3}}\\&+\frac{k_BT}{A^{1/3}r^{2/3}}+l_Bk_BT\nu^2K_0\left(\frac{r}{\lambda_D}\right)+l_Bk_BT\nu^2K_0\left(\frac{\pi r\tan\alpha}{\lambda_D}\right)-\frac{M}{r}\cos\alpha\end{aligned} \tag{21}$$

where $K_0(x)$ is a modified Bessel funtion, $A=\frac{K_b}{k_BT}$ is the bending persistence length, $C=\frac{K_t}{k_BT}$ is the twisting persistence length, l_B is the Bjerrum length, λ_D is the Debye length, ν is the effective charge per unit length [10] and M, the external moment, is determined by the force F acting on the DNA and the location s_1 at which we make the cut in the localizing solution. In fact, $M=FX(s_1)$ where $X(s_1)$ is the x-coordinate of the point at which we cut the localizing solution. In the above expression the first and second terms represent the elastic energy stored in the helices, the third and fourth term give the entropic cost of fluctuations of the rod around a helical shape and the fifth and sixth terms give the energy stored in the electrostatic interactions between the charged helices and ionic solution in which they are immersed. The Euler-Lagrange equations for equilibrium are

$$\frac{d}{ds}\frac{\partial \mathscr{L}}{\partial \alpha'} = \frac{\partial \mathscr{L}}{\partial \alpha}, \qquad \frac{d}{ds}\frac{\partial \mathscr{L}}{\partial \phi'} = \frac{\partial \mathscr{L}}{\partial \phi}. \tag{22}$$

The second of these equations says that $\phi' + \frac{\sin 2\alpha}{2r} = \kappa_3 = \frac{M_3}{K_t} = const$. The equation for α is obtained from the first of the Euler-Lagrange equations and is as follows:

$$\begin{aligned} K_b\alpha'' = &-\frac{2K_b}{r^2}\cos^3\alpha\sin\alpha + \frac{K_t}{r}(\phi' + \frac{1}{2r}\sin 2\alpha)\cos 2\alpha - \frac{2}{3}\frac{\pi k_B T r \sec^2\alpha}{A^{1/3}(\pi r\tan\alpha)^{5/3}} \\ &+ \frac{\pi r\sec^2\alpha}{\lambda_D} l_B k_B T \nu^2 K_0'\left(\frac{\pi r\tan\alpha}{\lambda_D}\right) + \frac{M}{r}\sin\alpha. \end{aligned} \tag{23}$$

For helices of constant pitch $\alpha'' = 0$ and hence we can rewrite the above equation as

$$\begin{aligned} &-\frac{2K_b}{r}\cos^3\alpha\sin\alpha + M_3\cos 2\alpha - \frac{2}{3}\left(\frac{r}{A}\right)^{1/3}\frac{k_B T}{\pi^{2/3}}\frac{\sec^2\alpha}{\tan^{5/3}\alpha} \\ &\quad - l_B k_B T \nu^2 \lambda_D K_1\left(\pi\frac{r}{\lambda_D}\tan\alpha\right)\frac{\pi r^2}{\lambda_D^2}\sec^2\alpha + M\sin\alpha = 0, \end{aligned} \tag{24}$$

where we have used the property of Bessel functions that $K_0'(x) = -K_1(x)$. This equation replaces eq.17 which was applicable only for the special case in which there are no interactions between the helices in the plectoneme. In the absence of any interactions between the helices the equation for α is

$$-\frac{2K_b}{r}\cos^3\alpha\sin\alpha + M_3\cos 2\alpha + M\sin\alpha = 0, \tag{25}$$

We expect that eq.17 (obtained from the balance of forces and moments) and eq.25 (obtained from the variational principle) should give the same solution for the plectonemic shape. We verify this in figure 2 where we compare the radius, number of turns and length of the helices in the plectoneme at the critical torque $\sqrt{2K_bF}$ [12] for different values of the force F and total length L. The length L is chosen to be large enough that we can assume $z_3 = 1$ without sacrificing the accuracy of the solution [15]. It is apparent from figure 2 that indeed both the variational approach and the balance of forces and moments approach give the same result. Interestingly, the radius of the plectoneme depends only on the tension F and not the length of the DNA while the length $2L_2$ eaten up by the plectonemic helices depends only on the length L of the DNA and not on the tension F as seen in figure 2(b). Therefore, the number of turns in the helix (see figure 2(c)) depends both on the tension F and the length L of the DNA in such a way as to ensure $2L_2$ is constant.

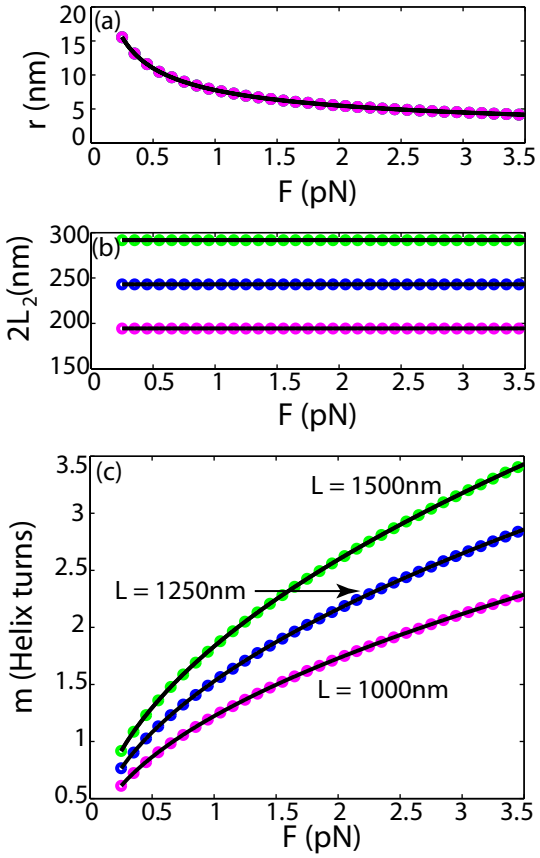

Fig. 2 Various parameters of the post-buckling plectoneme plotted as a function of the force F assuming no thermal fluctuations in a DNA fragment of length $L = 1000$nm (magenta), 1250nm (blue) and 1500nm (green). The colored circles are obtained by solving (17) while the solid black line passing through them is the result of solving (25) together with (13). (a) Radius of the plectonemic helix is independent of the length L. In fact, $r \propto F^{-1/2}$ (see Purohit (2008) [15]). (b) Length of the plectonemic helix is independent of the tension F. (c) The number of turns m in each of the helices of the plectoneme increases with increasing force. The calculations were performed assuming $K_b = 205\text{pNnm}^2$ and $K_t = 431\text{pNnm}^2$ which are typical of double-stranded DNA.

6 Configurational entropy and electrostatics in the plectoneme

At this point we also examine the effect of electrostatics and configurational entropy on the geometry of the plectonemic helices. The variational method allows us to do so in a straight forward manner as already illustrated above. We note (see figure 3(a)) that allowing the helices to fluctuate causes them to become shorter than the purely elastic helices. This is because the decrease of free energy (due to an increase of entropy) which could have been obtained by a small increase in the length of the helices is more than offset by the increase in the elastic energy. Since the fluctuations

become smaller with an increase in the tension we see that the length eaten up by the helices in the presence of fluctuations approaches the value obtained by the purely elastic treatment as the force becomes larger. Interestingly, electrostatics has a neglible impact on the geometry of the helices. The reason for this can be gleaned from figure 3(c) where we have plotted the elastic, entropic and electrostatic parts of the free energy density as a function of the radius of the plectonemic helices for a pitch angle $\alpha = 50$ degrees. It is evident that electrostatic energy is minuscule in comparison to the elastic part of the free energy.

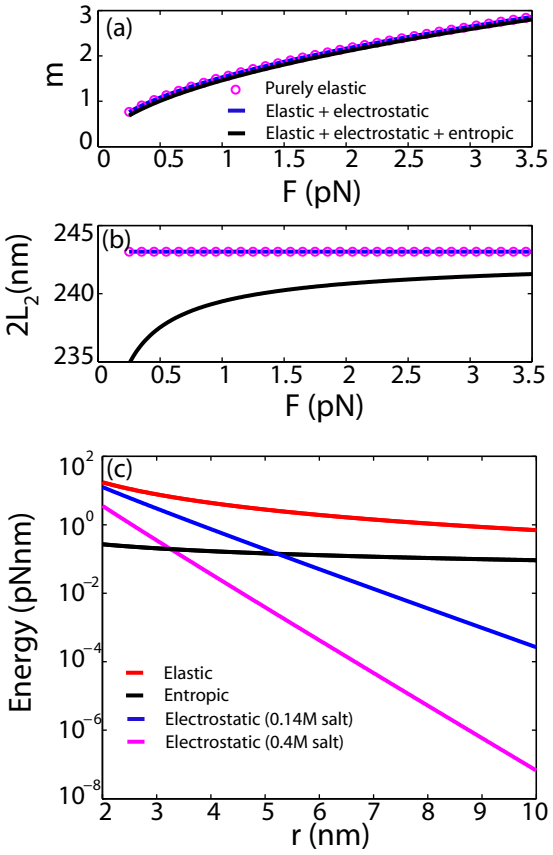

Fig. 3 The effect of electrostatics and thermal fluctuations (entropy) on the geometry of the plectonemic helices. (a) It is evident that electrostatics in 0.14M solution has practically no effect on the number of turns in the helices. (b) The length of the helices also remains practically unaffected by electrostatics. Fluctuations have a small effect as seen from the black line in both the figures. (c) The entropic and electrostatic part of the free energy are negligible in comparison to the elastic part of the free energy for values of helix radius $r > 5$nm. The electrostatic energy is larger for small ion concentrations because of lower screening of the negative charge on the DNA. The calculations were performed assuming $L = 1250$nm, $K_b = 205$pNnm^2 and $K_t = 431$pNnm^2 which are typical of double-stranded DNA.

We will now use eq.24 which gives equilibria of the plectoneme in the presence of elastic, entropic and electrostatic effects in conjunction with the equations describing the equilibria of a straight rod with elastic and entropic effects to obtain the shapes of the fluctuating DNA observed in the experiments of Forth *et al.* (2008) [6]. The expressions for the entropic elasticity of a straight twist-storing polymer, such as, DNA were given by Moroz and Nelson (1998) [12] and are rewritten below:

$$M_3(F,\Delta Lk) = \frac{2\pi\Delta Lk}{\frac{L}{K_t}+\frac{Lk_BT}{4K_b\sqrt{K_bF}}}, \tag{26}$$

$$\zeta(F,\Delta Lk) = 1-\frac{1}{2}\frac{1}{\sqrt{\frac{K_bF}{k_B^2T^2}-\frac{M_3^2}{4k_B^2T^2}-\frac{1}{32}}}+\frac{K_bk_BT}{L(K_bF-\frac{M_3^2}{4})}, \tag{27}$$

where $\zeta = \frac{Z(\frac{L}{2})-Z(-\frac{L}{2})}{L}$ is the non-dimensionalized extension, k_B is Boltzmann's constant and T is the absolute temperature. The above expressions are valid as long as $M_3 < 2\sqrt{K_bF}$ which, we recall, is the classical critical buckling torque in the zero temperature limit. We note that the classical expression for the torque $M_3 = K_t\frac{2\pi\Delta Lk}{L}$ in a straight rod is recovered from (26) when we set $T = 0$ which corresponds to no fluctuations. To couple the equations describing the plectoneme and those describing the straight rod we divide it into three regions – two largely straight but highly fluctuating regions each of length L_f corresponding to arc-length intervals $[-\frac{L}{2},-\frac{L_1}{2}]$ and $[\frac{L_1}{2},\frac{L}{2}]$, a highly curved region corresponding to $[-\frac{L_1}{2},\frac{L_1}{2}]$ with negligible fluctuations (Agrawal *et al.* (2008) [2] show that this is a reasonable assumption) and the plectonemic helices of length $4\pi mr\sec\alpha$. We follow exactly the same procedure as explained with the localizing solution for gluing these regions together. This leads to a system of equations consisting of (13), (24), (18) coupled with

$$\frac{M_3L}{2\pi K_t}+\frac{M_3L_fk_BT}{8\pi K_b\sqrt{K_bF}}+2m\sin\alpha = \Delta Lk, \tag{28}$$

$$L_f+L_1+4\pi mr\sec\alpha = L. \tag{29}$$

These are six equations for the seven unknowns – s_1, z_1, z_3, M_3, m, L_1 and L_f. We need one more condition to ensure that we have as many equations as there are unknowns. This last equation is obtained from the principle that the free energy of the equilibrium configuration should be a minimum. The required free energy is:

$$G = 4\pi mr\sec\alpha\mathscr{G}_{hel}+L_1\mathscr{G}_{rod}+L_f\mathscr{G}_{flc}-F(Z(+\frac{L}{2})-Z(-\frac{L}{2})), \tag{30}$$

where the free energy densities $\mathscr{G}_{hel}$, $\mathscr{G}_{rod}$ and $\mathscr{G}_{flc}$ are given by

$$\begin{aligned}\mathscr{G}_{hel} = {} & \frac{K_b}{2}\left(\alpha'^2+\frac{1}{r^2}\cos^4\alpha\right)+\frac{M_3^2}{2K_t}+\frac{k_BT}{A^{1/3}(\pi r\tan\alpha)^{2/3}}+\frac{k_BT}{A^{1/3}r^{2/3}}\\ & +l_Bk_BT\nu^2K_0\left(\frac{r}{\lambda_D}\right)+l_Bk_BT\nu^2K_0\left(\frac{\pi r\tan\alpha}{\lambda_D}\right)-\frac{M}{r}\cos\alpha,\end{aligned} \tag{31}$$

$$\mathscr{G}_{rod} = \frac{F}{2}(1+z_1+z_3-z_1z_3)+\frac{M_3^2}{2K_t}+F\frac{Z(+\frac{L_1}{2})-Z(-\frac{L_1}{2})}{L_1}, \tag{32}$$

$$\mathscr{G}_{flc} = -k_BT\frac{Pk_BT}{K_b}(1-\frac{1}{4P}-\frac{1}{64P^2})+\frac{M_3^2}{2K_t}, \tag{33}$$

where $P=\frac{\sqrt{K_bF-\frac{M_3^2}{4}}}{k_BT}$. The rest of the calculation is performed as in Purohit (2008) [15]. The resulting dependence of the end-to-end distance $Z(\frac{L}{2})-Z(-\frac{L}{2})$ on the link added at the ends is shown in figure 4(a). The jump in the end-to-end extension at a critical number of turns is seen here as in the experiment of Forth *et al.* (2008) [6]. The linear decrease in the end-to-end extension with an increase in the added link is also reproduced. Furthermore, the torque M_3 felt at the ends $s=\pm\frac{L}{2}$ is plotted in figure 4(b) and its dependence on the number of turns added is similar to that seen in the experiments. There is a linear rise in the beginning but there is a plateau after plectoneme formation has occurred. This is similar to the observations in the experiments of Forth *et al.* (2008) [6]. Thus all the qualitative features of rotation-extension curves are reproduced by our theory.

We now turn to a quantitative comparison between theory and experiment. The slope of the linear rotation-extension plot after plectoneme formation is known to be independent of the length of DNA in the experiment [11, 3]. We verify that this is indeed the case in Figure 5(a) by plotting the rotation-extension curve for three different lengths and the same bending and twisting moduli and electrostatic parameters. One of the lengths ($L=1430$nm) is the length of DNA used in the experiments of Forth *et al.* (2008) [6]. We use the bending and twisting modulus inferred from the experiments of Forth *et al.* (2008) [6]. However, the slope of our rotation-extension curve (61.3nm per turn) is very different from that obtained from the experiments of Forth *et al.* (2008) [6] (about 30nm per turn). In order to understand the reason for this discrepancy we plot the post-plectoneme slope as a function of twisting modulus keeping all other parameters fixed in figure 5(b) and repeat the exercise with the bending modulus in figure 5(c). We find that the post plectoneme slope is independent of the twisting modulus and decreases with a decreasing bending modulus. This seems to suggest that there is some softening in the DNA when plectonemes are formed. The reason for the softening could be a loss of structural integrity in the DNA due to the small radii of curvature produced in the plectonemes (see figure 2(a) while remembering that the diameter of DNA is about 2nm). In fact, lower moduli have been reported by Cloutier and Widom (2005) [4] for cyclization of short DNA fragments where small radii of curvature are produced.

7 Conclusions

In this paper we have coupled the equations describing the entropic elasticity of a fluctuating rod with a variational formulation describing plectonemes to understand

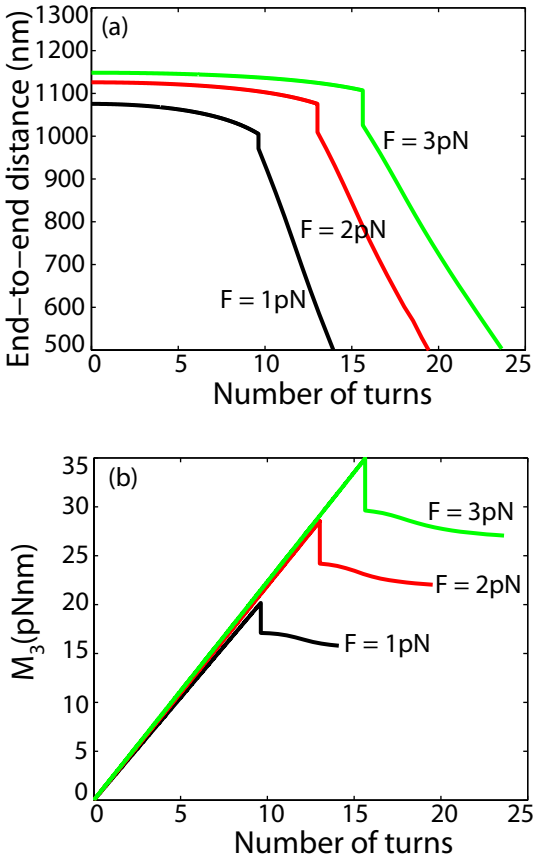

Fig. 4 The end-to-end distance $Z(L/2) - Z(-L/2)$ and the torque M_3 are plotted as a function of the number of turns applied to the DNA. Thermal fluctuations, electrostatics and elasticity are all included in this calculation. The trends observed in the plots are similar to those in the experiment of Forth *et al.* (2008) [6]. The calculations were performed assuming $L = 1250$nm, $K_b = 205$pNnm^2 and $K_t = 431$pNnm^2 which are typical of double-stranded DNA. The salt concentration is assumed to be 0.14M.

the mechanics of plectonemes in DNA. We have shown that configurational entropy plays a more significant role compared to electrostatics (with monovalent counterions) in describing the shapes of twisted fluctuating DNA. We have also shown that the variational method and a solution to the equations for the balance of forces and moments in a rod give the same parameters for the plectoneme. The variational method, however, is more general since it can be easily extended to account for various types of interactions in the DNA that would be difficult to model in the other approach. We also found that the slope of the rotation-extension curve is unaffected by the length of the DNA and its twisting modulus and decreases with a decreasing bending modulus.

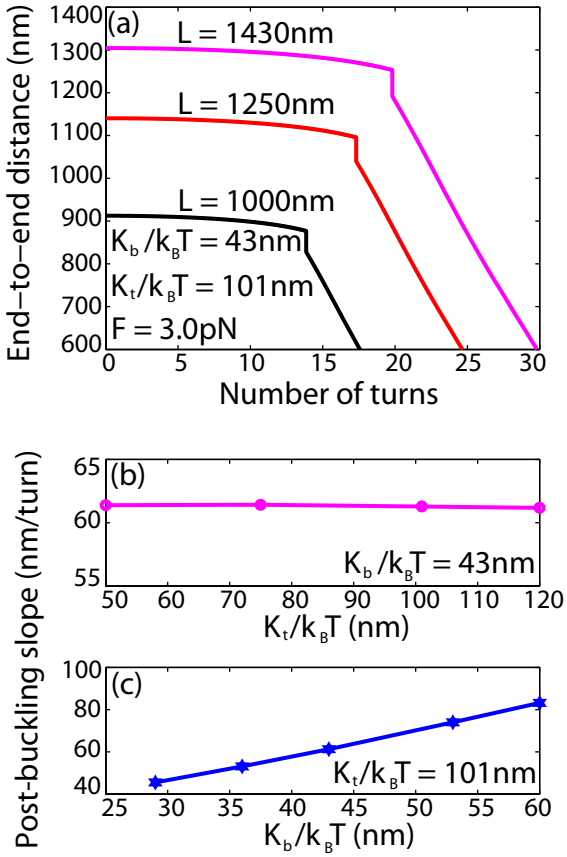

Fig. 5 Comparison with experiments. (a) The end-to-end distance $Z(L/2) - Z(-L/2)$ at $F = 3.0$pN is plotted as a function of the number of turns applied to DNA of three different lengths – 1000nm, 1250nm and 1430nm. Of these $L = 1430$nm is one of the lengths in the experiments of Forth *et al.* (2008) [6]. The calculations were performed assuming $K_b = 175\text{pNnm}^2$ and $K_t = 411\text{pNnm}^2$ which were deduced from measurements by Forth *et al.* (2008) [6]. The salt concentration is assumed to be 0.14M. We get a slope of about 61.3nm per turn in the post-plectoneme region irrespective of the length of the DNA. The slope in the experiment is about 30nm per turn. (b) We keep the bending modulus constant at $K_b = 175\text{pNnm}^2$ and plot the post-plectoneme slope as a function of the twisting modulus. We see that the slope does not depend on the twisting modulus. (c) Here we keep the twisting modulus constant at $K_t = 411\text{pNnm}^2$ and plot the slope as a function of the bending modulus. We find that low slopes in the rotation-extension plots are a result of lower bending moduli.

References

1. Abramowitz M, Stegun IA (1964) Handbook of Mathematical functions, National Bureau of Standards, Washington D.C.
2. Agrawal NJ, Radhakrishnan R, Purohit PK, (2008) Geometry of mediating protein affects the probability of loop formation in DNA. Biophys J 94:3150–3158.

3. Clauvelin N, Audoly B, Neukirch S (2008) Mechanical response of plectonemic DNA: An analytical solution. Macromolecules 41(12):4479–4483. .
4. Cloutier TE, Widom J (2005) DNA twisting flexibility and the formation of sharply looped protein-DNA complexes. Proc. Natl. Acad. Sci. USA 102:3645–3650.
5. Coleman BD, Swigon D, Tobias I (2000) Elastic stability of DNA configurations. II. Supercoiled plasmids with self-contact. Phys. Rev. E 61:759–770.
6. Forth S, Deufel C, Sheinin MY, Daniels B, Sethna JP, Wang MD (2008) Abrupt buckling transition observed during the plectoneme formation of individual molecules. Phys. Rev Lett 100: 148301.
7. Fuller FB (1971) The writhing number of a space curve. Proc. Natl. Acad. Sci. USA 68:815–819.
8. Goyal S, Perkins NC, Lee CL (2008) Non-linear dynamic intertwining of rods with self-contact. Intl. J. Nonlin. Mech. 43(1):65–73.
9. Marko JF and Siggia ED (1995) Stretching DNA. Macromolecules 28:8759–8770.
10. Marko JF and Siggia ED (1995) Statistical mechanics of supercoiled DNA. Phys. Rev. E 52(3):2912–2938.
11. Marko JF (2007) Torque and dynamics of linking number relaxation in stretched supercoiled DNA. Phys. Rev. E 76(2):021926.
12. Moroz JD, Nelson PC (1998) Entropic elasticity of twist storing polymers. Macromolecules 31:6333–6347.
13. Nizette M and Goriely A (1999) Towards a classification of Euler-Kirchhoff filaments. J. Math. Phys. 40(6):2830–2866.
14. Purohit PK, Nelson PC (2006) Effect of supercoiling on formation of protein mediated DNA loops. Phys. Rev. E 74:061907.
15. Purohit PK (2008) Plectoneme formation in twisted fluctuating rods. J. Mech. Phys. Solids 56:1715–1729.
16. Stump DM, Fraser WB, Gates KE (1998) The writhing of circular cross-section rods: undersea cables to DNA supercoils. Proc. R. Soc. Lond. A 454:2123–2156.
17. Stump DM, Fraser WB (2000) Multiple solutions for writhed rods: implications for DNA supercoiling. Proc. R. Soc. Lond. A 456:455–467.
18. van der Heijden GHM, Thompson JMT, Neukirch S (2003) A variational approach to loaded ply structures. J. Vibration and Control 9:175–185.
19. van der Heijden GHM, Peletier MA, Planque R (2006) Self-contact for rods on cylinders. Arch. Rational Mech. Anal. 182:471–511.